ISSN: 2769-545X

Research Article

Advances in Machine Learning & Artificial Intelligence

Covariance Eigenanalysis for Direction Finding with Analytic Ray-Traced Steering Vectors

Greg Passmore*

PassmoreLab, Austin, Texas, USA

***Corresponding Author**
Greg Passmore, PassmoreLab, Austin, Texas, USA.

Submitted: 2026, Feb 13; **Accepted**: 2026, Mar 24; **Published**: 2026, Apr 17

Citation: Passmore, G. (2026). Covariance Eigenanalysis for Direction Finding with Analytic Ray-Traced Steering Vectors. *Adv Mach Lear Art Inte, 7*(2), 01-35.

Abstract

In our setup of multiple phased array antennas, the goal was to replicate current techniques for object location. For this, we incorporated Multiple Signal Classification (MUSIC), a subspace DOA estimator for multiple narrowband sources impinging on our phased arrays. This is based on the eigendecomposition of the sample spatial covariance $\hat{\mathbf{R}}$ *and the resulting partition of* $\mathbb{C}^M$ *into orthogonal signal and noise subspaces. Candidate directions are evaluated by the noise-subspace projection energy* $d(theta) = ||Un^H a(theta)||_2^2$*, and DOA hypotheses are taken from peaks of the reciprocal pseudospectrum* $P_{\text{MUSIC}}(\theta) = d(\theta)^{-1}$.

Here a(θ) is generated by our analytic ray tracer rather than a typical ideal plane-wave model. For each scan direction, the ray tracer returns the per-element complex field after integrating refractive optical path length and attenuation along the propagation path to each sensor, with optional instrument phase and gain terms. MUSIC is then applied, but steering-vector mismatch from refraction and loss is moved from an unmodeled error term into the forward model used inside d(θ).

This combination provides several operational advantages. MUSIC preserves super-resolution angular discrimination by exploiting covariance eigenstructure rather than relying on beamwidth-limited steering. Ray tracing reduces deterministic bias by ensuring the steering vector includes atmospheric refraction and absorption, preventing these effects from being absorbed into noise-subspace leakage. The result is a DOA estimator that remains mathematically identical to standard MUSIC, but produces bearings that are physically consistent under non-ideal propagation conditions, improving downstream fusion stability and track repeatability.

The development proceeds from the narrowband array model through finite-snapshot covariance estimation and Hermitian eigenanalysis to an explicit summation-form master equation that maps directly to loop-based implementations. The same algebra is retained when the steering vector is replaced by ray-integrated propagation, enabling a propagation-aware pseudospectrum evaluation under refracting and lossy atmospheres.

Keywords: Direction-Of-Arrival Estimation, MUSIC Algorithm, Covariance Eigenanalysis, Ray-Traced Steering Vectors, Atmospheric Propagation Modeling

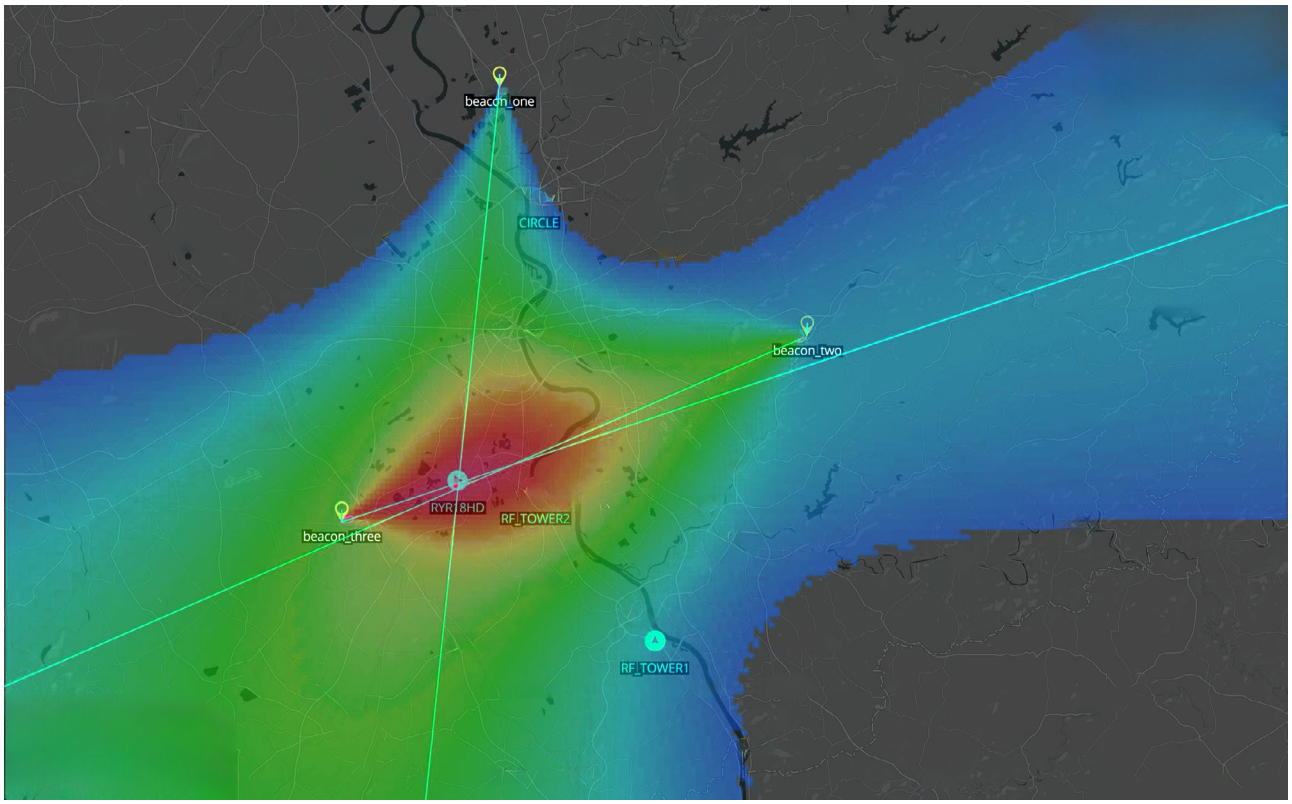

1. Introduction

Direction-of-arrival (DOA) estimation uses spatial phase and amplitude structure across a receiving array to infer the bearings of one or more emitters. In multi-emitter conditions the measured snapshot vectors contain overlapping spatial signatures that are perturbed by thermal noise, interference, finite-snapshot covariance error, and array calibration mismatch. The result is that the bearing information is present but not separable by direct per-sensor inspection, and estimation performance is often dominated by model mismatch rather than by aperture alone.

MUSIC addresses this regime by exploiting the eigenstructure of the spatial covariance estimate $\hat{\mathbf{R}}$. Under the standard narrowband model, the dominant eigenspace spans the signal subspace, while the remaining eigenspace spans a noise subspace that is orthogonal to the signal component. DOA estimation is implemented as a search over candidate steering vectors, where directions consistent with the signal subspace minimize the noise-subspace projection energy and therefore maximize $P_{\mathrm{MUSIC}}(\theta)$.

This paper presents MUSIC in an implementation-oriented form and then replaces the conventional plane-wave steering model with a ray-traced steering operator. The ray tracer supplies $\mathrm{a}(\theta)$ by integrating refractive index and attenuation along sensor-dependent paths, producing a complex steering vector whose phase and amplitude are consistent with the environment and calibrated receiver response. The remaining steps (covariance construction, eigenvalue sorting, noise-subspace projection, and scan-grid peak selection) are unchanged, but the hypothesis test is applied to a forward model that reflects propagation physics rather than a geometric far-field approximation.

2. Background and Historical Context

MUSIC was introduced as an eigenstructure-based approach to resolving multiple emitters beyond the mainlobe resolution limits of conventional beamforming [1]. Its core mechanism, using orthogonality between a noise subspace and steering vectors associated with true sources, is closely related to earlier eigenanalysis approaches in spectral estimation such as Pisarenko harmonic decomposition [2]. Subsequent work established the optimality of eigensystem-based high-resolution methods and analyzed the statistical behavior of subspace estimators under finite-sample covariance error, establishing bounds and comparisons to maximum-likelihood estimators, while comprehensive treatments of array processing assumptions and covariance structure are provided in standard references [3-5].

MUSIC remains operationally relevant because it separates the estimation problem into two parts with clear control variables: covariance estimation quality (snapshot count, interference conditions, calibration) and forward-model accuracy in the steering vector used during

the scan. In many practical systems, performance degradation is dominated by steering mismatch rather than by eigenanalysis itself. This motivates treating the steering vector as a propagation operator, so that refraction and loss enter as modeled terms rather than residual error.

2.1. Value in Tracking

A DOA output from MUSIC can be paired with a covariance-derived uncertainty proxy and inserted directly into tracking updates. One practical proxy is the local curvature of log $P_{\mathrm{MUSIC}}(\theta)$ at a detected peak, which provides a bearing-variance scale that maps naturally to the measurement noise term $R = \sigma_\theta^2$ in a bearing-only filter. In addition, eigenvalue separation between the signal eigenvalues and the noise cluster provides a data-driven indicator of subspace stability, which correlates with the sensitivity of peak location to snapshot resampling and small perturbations of $\hat{\mathbf{R}}$.

When steering vectors are ray-traced, these confidence quantities can be interpreted more cleanly. A loss of peak sharpness can be associated with either reduced SNR / snapshot support in $\hat{\mathbf{R}}$ or with residual propagation mismatch after the ray model is applied. This separation is useful in tracking and sensor management because it distinguishes data-limited uncertainty from model-limited uncertainty and supports explicit tuning of $\eta_m(\theta)$ or related mismatch parameters.

3. Relationship with CID, TC and TQ

In CID workflows, DOA estimates act as geometric constraints that reduce association ambiguity and improve multi-sensor fusion. The bearing estimate $\hat{\theta}$ and its variance σ_θ^2 enter as measurement and measurement noise in standard filters, tightening the posterior covariance and increasing track quality (TQ) when the geometry is informative. Over time, repeatability of bearings and stability of peak structure provide evidence that the emitter is persistent and not attributable to transient interference, supporting target confidence (TC) through likelihood consistency.

Ray-traced steering vectors strengthen this linkage by reducing systematic bias caused by unmodeled propagation. When refraction and attenuation are incorporated into $a(\theta)$, the residual bearing error is less dominated by deterministic mismatch and more dominated by stochastic terms that can be parameterized. This tends to improve the interpretation of σ_θ^2 as an actual measurement variance for downstream fusion rather than as a proxy contaminated by unmodeled steering error.

4. Advantages of this Approach

The steering vector is generalized from a geometric plane-wave phase progression to a propagation operator defined by ray-integrated phase and attenuation along the path to each sensor. For each candidate direction, the complex field is constructed from path integrals of refractive index and specific attenuation, together with calibrated element gain and instrument phase. This replaces the idealized spatial exponential with a physically propagated response while preserving the algebra of the MUSIC projection. The covariance eigendecomposition and noise-subspace partition remain unchanged; only the forward model embedded in a(θ) is modified. Any remaining discrepancy between modeled and measured propagation is isolated explicitly as a residual complex perturbation $\eta_m(\theta)$, separating deterministic environmental effects from stochastic mismatch.

5. Notation Used

Symbol	Type / Dimension	Description
M	Scalar (int)	Number of antenna elements in the array
K	Scalar (int)	Number of incident sources (true model order), with $K < M$
$\hat{K}$	Scalar (int)	Estimated number of sources used for subspace partitioning
N	Scalar (int)	Number of snapshots used to form the sample covariance
Θ	Set	DOA scan grid of candidate angles
θ	Scalar (rad or deg)	Hypothesized scan angle
θ_k	Scalar (rad or deg)	True direction of arrival for source k
k	Index	Source index, $k = 1, \ldots, K$
m	Index	Antenna index, $m = 1, \ldots, M$
n	Index	Snapshot index, $n = 1, \ldots, N$
r	Index	Noise-subspace eigenvector index, $r = 1, \ldots, M - \hat{K}$
i, j, p	Index	Antenna indices used in covariance and expanded sums
$x_m(n)$	Complex scalar	Complex baseband sample (IQ) from antenna m at snapshot n
$\mathbf{x}(n)$	$\mathbb{C}^{M\times 1}$	Snapshot vector $[x_1(n), \ldots, x_M(n)]^T$
$s_k(n)$	Complex scalar	Source waveform for source k at snapshot n
$\mathbf{s}(n)$	$\mathbb{C}^{K\times 1}$	Source vector $[s_1(n), \ldots, s_K(n)]^T$
$\mathbf{w}(n)$	$\mathbb{C}^{M\times 1}$	Additive noise vector at snapshot n
σ^2	Real scalar	Spatially white noise variance
$\mathbf{I}$	$\mathbb{R}^{M\times M}$	Identity matrix
$\mathcal{CN}(\mathbf{0}, \sigma^2\mathbf{I})$	Distribution	Circular complex Gaussian noise model
$\mathbf{a}(\theta)$	$\mathbb{C}^{M\times 1}$	Steering vector for a hypothesized direction θ
$a_m(\theta)$	Complex scalar	Steering vector component for antenna m
$\mathbf{A}$	$\mathbb{C}^{M\times K}$	Steering matrix $[\mathbf{a}(\theta_1) \ldots \mathbf{a}(\theta_K)]$
$\mathbf{R}$	$\mathbb{C}^{M\times M}$	True spatial covariance $\mathbb{E}\{\mathbf{x}\mathbf{x}^H\}$
$\hat{\mathbf{R}}$	$\mathbb{C}^{M\times M}$	Sample covariance $\frac{1}{N}\sum_{n=1}^{N}\mathbf{x}(n)\mathbf{x}^H(n)$
$\hat{R}_{ij}$	Complex scalar	Sample covariance entry (i, j)
$\mathbf{R}_s$	$\mathbb{C}^{K\times K}$	Source covariance $\mathbb{E}\{\mathbf{s}\mathbf{s}^H\}$

$\mathbf{U}$	$\mathbb{C}^{M\times M}$	Unitary eigenvector matrix of $\mathbf{R}$ or $\hat{\mathbf{R}}$
$\mathbf{u}_m$	$\mathbb{C}^{M\times 1}$	Eigenvector (column of $\mathbf{U}$)
$\mathbf{\Lambda}$	$\mathbb{R}^{M\times M}$	Diagonal eigenvalue matrix $\mathrm{diag}(\lambda_1,\ldots,\lambda_M)$
λ_ℓ	Real scalar	Eigenvalue ℓ of $\mathbf{R}$ or $\hat{\mathbf{R}}$
$\mathbf{U}_s$	$\mathbb{C}^{M\times K}$	Signal-subspace eigenvector matrix (largest K eigenvalues)
$\mathbf{U}_n$	$\mathbb{C}^{M\times(M-\hat{K})}$	Noise-subspace eigenvector matrix (smallest $M-\hat{K}$ eigenvalues)
$u_{m,r}$	Complex scalar	Entry of $\mathbf{U}_n$ at antenna m, noise mode r
$\mathbf{\Lambda}_n$	$\mathbb{R}^{(M-\hat{K})\times(M-\hat{K})}$	Diagonal noise-subspace eigenvalue matrix
$\mathbf{c}_k$	$\mathbb{C}^{K\times 1}$	Coefficients such that $\mathbf{a}(\theta_k)=\mathbf{U}_s\mathbf{c}_k$
$\mathbf{y}(\theta)$	$\mathbb{C}^{(M-\hat{K})\times 1}$	Noise-subspace projection $\mathbf{U}_n^H\mathbf{a}(\theta)$
$y_r(\theta)$	Complex scalar	Noise-mode projection coefficient $\sum_{m=1}^{M} u_{m,r}^* a_m(\theta)$
$d(\theta)$	Real scalar	Projection energy denominator $d(\theta)=\lVert\mathbf{U}_n^H\mathbf{a}(\theta)\rVert_2^2$
$P(\theta)$	Real scalar	Pseudospectrum value $P(\theta)=d(\theta)^{-1}$
$P_{\mathrm{MUSIC}}(\theta)$	Real scalar	MUSIC pseudospectrum (explicitly named form of $P(\theta)$)
ϵ	Small positive scalar	Numerical floor used to avoid division by zero
$\hat{\theta}$	Scalar (rad or deg)	Estimated DOA from $\arg\max_{\theta\in\Theta} P(\theta)$
$\hat{\sigma}_\theta^2$	Real scalar	Local curvature-based bearing variance proxy
$\frac{d^2}{d\theta^2}\log P(\theta)$	Real scalar	Second derivative of log-pseudospectrum used for curvature-based uncertainty
z	Scalar (rad or deg)	Bearing observation used in tracking, typically $z=\hat{\theta}$
v	Scalar	Bearing measurement noise, $v\sim\mathcal{N}(0,\sigma_\theta^2)$
σ_θ^2	Real scalar	Bearing measurement variance used in tracking (often $\hat{\sigma}_\theta^2$)
R	Real scalar or matrix	Measurement noise variance/covariance (bearing-only case: $R=\sigma_\theta^2$)
$\mathbf{x}$	$\mathbb{R}^{2\times 1}$	Target position state $[x,y]^T$ (CID planar model)
$\mathbf{s}$	$\mathbb{R}^{2\times 1}$	Receiver position $[s_x,s_y]^T$ (single node)
$h(\mathbf{x})$	Scalar	Bearing function $\mathrm{atan2}(y-s_y,x-s_x)$
$\Delta x,\Delta y$	Real scalars	Relative coordinates $\Delta x=x-s_x$, $\Delta y=y-s_y$
r^2	Real scalar	Range-squared $r^2=\Delta x^2+\Delta y^2$
$\mathbf{H}$	$\mathbb{R}^{1\times 2}$	Jacobian of bearing model $[-\Delta y/r^2,\ \Delta x/r^2]$

$\mathbf{x}^-, \mathbf{x}^+$	State vectors	Prior and posterior track state (EKF notation)
$\mathbf{P}^-, \mathbf{P}^+$	Covariance matrices	Prior and posterior track covariance
$\tilde{y}$	Scalar	Innovation residual $\tilde{y} = z - h(\mathbf{x}^-)$
S	Real scalar	Innovation variance $S = \mathbf{H}\mathbf{P}^-\mathbf{H}^T + R$
$\mathbf{K}$	Gain vector	Kalman gain $\mathbf{K} = \mathbf{P}^-\mathbf{H}^T S^{-1}$
EPE	Real scalar	Equivalent position error proxy $\sqrt{\mathrm{trace}(\mathbf{P}^+)}$ (as defined)
τ	Real scalar	Scale parameter in $\mathrm{TQ} = \exp(-\mathrm{EPE}^2/\tau^2)$
TQ	Real scalar	Track quality score derived from posterior covariance
I	Scalar (int)	Number of bearing nodes used in multi-node fusion
$(s_{x,i}, s_{y,i})$	Real scalars	Position of node i
z_i	Scalar (rad or deg)	Bearing measurement from node i
$\mathbf{u}_i$	$\mathbb{R}^{2\times 1}$	Bearing direction unit vector $[\cos z_i,\ \sin z_i]^T$
$\mathbf{n}_i$	$\mathbb{R}^{2\times 1}$	Perpendicular unit vector $[-\sin z_i,\ \cos z_i]^T$
$\mathbf{A}$ (LS)	$\mathbb{R}^{I\times 2}$	Least-squares line-constraint matrix built from z_i
$\mathbf{b}$	$\mathbb{R}^{I\times 1}$	Least-squares right-hand side built from node positions
w_i	Real scalar	Bearing weight $w_i = \sigma_{\theta,i}^{-2}$
$\mathbf{W}$	$\mathbb{R}^{I\times I}$	Diagonal weight matrix $\mathrm{diag}(w_1, \ldots, w_I)$
$\hat{\mathbf{x}}$	$\mathbb{R}^{2\times 1}$	Weighted least-squares geolocation estimate
$\mathbf{P}_{\mathrm{LS}}$	$\mathbb{R}^{2\times 2}$	Approximate LS covariance $(\mathbf{A}^T\mathbf{W}\mathbf{A})^{-1}$
H	Hypothesis	Target-of-interest hypothesis used in TC
$\bar{H}$	Hypothesis	Competing hypothesis (not-of-interest)
r_i	Scalar	Bearing residual $r_i = \mathrm{wrap}(z_i - \theta_i^-(H))$
$\theta_i^-(H)$	Scalar	Predicted bearing at node i under hypothesis H
$\bar{r}_i$	Scalar	Bearing residual under $\bar{H}$ model
$\bar{\sigma}_{\theta,i}^2$	Real scalar	Bearing variance used under $\bar{H}$ model
$p(\mathbf{z} \mid H)$	Likelihood	Measurement likelihood under H
$\mathbf{z}$	Vector	Stacked bearings $[z_1, \ldots, z_I]^T$
$\mathcal{L}$	Real scalar	Log-likelihood ratio for TC

$P(H)$	Real scalar	Prior probability of hypothesis H
$P(\bar{H})$	Real scalar	Prior probability of hypothesis $\bar{H}$
TC	Real scalar	Target confidence posterior probability
d	Real scalar	ULA inter-element spacing
λ	Real scalar	Wavelength
k	Real scalar	Spatial frequency $k = 2\pi/\lambda$
j	Imaginary unit	$j = \sqrt{-1}$
$(\cdot)^T$	Operator	Transpose
$(\cdot)^H$	Operator	Hermitian (conjugate transpose)
$(\cdot)^*$	Operator	Complex conjugation
$\|\cdot\|_2$	Operator	Euclidean norm
$\mathrm{trace}(\cdot)$	Operator	Matrix trace
$\det(\cdot)$	Operator	Determinant
$\arg\max$	Operator	Maximizer operator over the scan grid
$\mathrm{atan2}(\cdot,\cdot)$	Function	Two-argument arctangent producing a signed angle
$\mathrm{wrap}(\cdot)$	Function	Angle wrapping to a principal interval (implementation-defined)
$\mathbf{s}_m$	$\mathbb{R}^{3\times1}$	Position vector of sensor element m in 3D space
$\hat{\mathbf{u}}(\theta)$	$\mathbb{R}^{3\times1}$	Unit direction vector corresponding to scan angle θ
$\mathbf{r}_m(\ell;\theta)$	$\mathbb{R}^{3\times1}$	Ray trajectory to sensor m parameterized by arc length ℓ
ℓ	Real scalar	Ray path arc-length parameter
$L_m(\theta)$	Real scalar	Total ray path length to sensor m for scan direction θ
$\hat{\mathbf{t}}_m(\ell;\theta)$	$\mathbb{R}^{3\times1}$	Unit tangent vector to the ray path at ℓ
ω_0	Real scalar (rad/s)	Carrier angular frequency
c	Real scalar	Speed of light in vacuum
k_0	Real scalar	Free-space wavenumber $k_0 = \omega_0/c$
$n(\mathbf{r},t)$	Real scalar field	Refractive index field as a function of position and time
$\Delta n(\mathbf{r},t)$	Real scalar field	Refractivity perturbation such that $n = 1 + \Delta n$
∇n	$\mathbb{R}^{3\times1}$	Spatial gradient of refractive index
$\alpha(\mathbf{r},t)$	Real scalar field	Specific attenuation coefficient (nepers/m)
$G_m(\theta)$	Complex scalar	Calibrated complex element gain/pattern response for sensor m

$\Phi_m(\theta)$	Real scalar (rad)	Accumulated propagation phase along ray to sensor m
$\mathcal{A}_m(\theta)$	Real scalar	Accumulated attenuation integral along ray to sensor m
$\phi_{m,\text{inst}}$	Real scalar (rad)	Instrument phase offset for sensor m
$a_{m,\text{inst}}$	Real scalar	Instrument amplitude-loss term for sensor m
$\eta_m(\theta)$	Complex random scalar	Residual complex perturbation (scintillation/mismatch) for sensor m
$\sigma^2_{\eta,m}$	Real scalar	Variance of residual complex perturbation $\eta_m(\theta)$
$\bar{a}_m(\theta)$	Complex scalar	Deterministic ray-traced steering component without residual perturbation
$\bar{y}_r(\theta)$	Complex scalar	Deterministic noise-subspace projection coefficient
$\Delta y_r(\theta)$	Complex scalar	Random perturbation term in noise-subspace projection coefficient
$I_{n,m}(\theta;t)$	Real scalar	Ray integral of refractive index $\int_0^{L_m(\theta)} n(\mathbf{r}_m(\ell;\theta),t)d\ell$
$I_{\alpha,m}(\theta;t)$	Real scalar	Ray integral of attenuation $\int_0^{L_m(\theta)} \alpha(\mathbf{r}_m(\ell;\theta),t)d\ell$
t	Real scalar	Time parameter used for time-varying atmosphere fields
s	Real scalar	Arc-length variable used in ray differential equations

6. Breakout for CID

A subspace DOA estimator provides a bearing measurement with an associated uncertainty. In CID, this bearing is treated as an observation that constrains target location, improves track quality through Bayesian filtering, and contributes to target confidence through likelihood-based evidence accumulation.

6.1. DOA Measurement Produced by The Subspace Estimator

Let the scan grid be θ and define the pseudospectrum

$$P(\theta) = \left[\mathbf{a}^H(\theta)\mathbf{U}_n\mathbf{U}_n^H\mathbf{a}(\theta)\right]^{-1}$$

A bearing estimate is obtained as the peak location

$$\hat{\theta} = \arg\max_{\theta\in\Theta} P(\theta)$$

A local curvature-based bearing variance can be defined from the second derivative of the log spectrum at the peak:

$$\hat{\sigma}^2_{\hat{\theta}} \approx \left[-\frac{d^2}{d\theta^2}\log P(\theta)\Big|_{\theta=\hat{\theta}}\right]^{-1}$$

This yields a measurement and an uncertainty pair $(\hat{\theta}, \hat{\sigma}^2_{\hat{\theta}})$ that can be inserted into CID tracking and confidence logic.

6.2. Bearing-Only Observation Model for A Single Receiving Node

Let the target state in a planar CID map be

$$\mathbf{x} = \begin{bmatrix} x \\ y \end{bmatrix}$$

Let the receiving node (array) position be

$$\mathbf{s} = \begin{bmatrix} s_x \\ s_y \end{bmatrix}$$

The predicted bearing from node to target is

$$h(\mathbf{x}) = \operatorname{atan2}(y - s_y,\, x - s_x)$$

The bearing measurement equation is

$$z = h(\mathbf{x}) + v, \quad v \sim \mathcal{N}(0, \sigma_\theta^2)$$

where $z = \hat{\theta}$ and $\sigma_\theta^2 = \hat{\sigma}_\theta^2$.

6.3. Linearization and Jacobian

Define

$$\Delta x = x - s_x, \quad \Delta y = y - s_y, \quad r^2 = \Delta x^2 + \Delta y^2$$

The Jacobian of the bearing function with respect to target position is

$$\mathbf{H} = \frac{\partial h}{\partial \mathbf{x}} = \begin{bmatrix} \frac{\partial h}{\partial x} & \frac{\partial h}{\partial y} \end{bmatrix} = \begin{bmatrix} -\frac{\Delta y}{r^2} & \frac{\Delta x}{r^2} \end{bmatrix}$$

This Jacobian explicitly shows that bearing information weakens as range grows (via $1/r^2$).

6.4. Track-Quality Update via EKF

Assume a prior track estimate ($\mathbf{x}^-$,$\mathbf{P}^-$).

Innovation:

$$\tilde{y} = z - h(\mathbf{x}^-)$$

Innovation covariance (scalar for bearing-only):

$$S = \mathbf{H}\mathbf{P}^-\mathbf{H}^T + R$$

With $R = \sigma_\theta^2$.
Kalman gain:

$$\mathbf{K} = \mathbf{P}^-\mathbf{H}^T S^{-1}$$

State update:

$$\mathbf{x}^+ = \mathbf{x}^- + \mathbf{K}\tilde{y}$$

Covariance update:

$$\mathbf{P}^+ = (\mathbf{I} - \mathbf{K}\mathbf{H})\mathbf{P}^-$$

Track quality (TQ) is typically derived from $\mathbf{P}^{+}$, for example by an equivalent position error measure:

$$\mathrm{EPE} = \sqrt{\mathrm{trace}(\mathbf{P}^{+})}$$

and a monotone mapping to a bounded score:

$$\mathrm{TQ} = \exp\left(-\frac{\mathrm{EPE}^2}{\tau^2}\right)$$

where τ is a chosen scaling parameter.

6.5. Direct Geolocation from Multiple Bearing Nodes

For node i at position $(s_{x,i}, s_{y,i})$ with bearing $z_i = \hat{\theta}_i$, define the unit direction vector

$$\mathbf{u}_i = \begin{bmatrix} \cos z_i \\ \sin z_i \end{bmatrix}$$

and the perpendicular unit vector

$$\mathbf{n}_i = \begin{bmatrix} -\sin z_i \\ \cos z_i \end{bmatrix}$$

A target point $\mathbf{x}$ lying on the bearing line satisfies

$$\mathbf{n}_i^T(\mathbf{x} - \mathbf{s}_i) = 0$$

Expanding:

$$(-\sin z_i)(x - s_{x,i}) + (\cos z_i)(y - s_{y,i}) = 0$$

Rearrange into linear form in (x, y):

$$(-\sin z_i)x + (\cos z_i)y = (-\sin z_i)s_{x,i} + (\cos z_i)s_{y,i}$$

Stacking I bearing equations yields

$$\mathbf{A}\mathbf{x} = \mathbf{b}$$

with

$$\mathbf{A} = \begin{bmatrix} -\sin z_1 & \cos z_1 \\ -\sin z_2 & \cos z_2 \\ \vdots & \vdots \\ -\sin z_I & \cos z_I \end{bmatrix}, \quad \mathbf{b} = \begin{bmatrix} (-\sin z_1)s_{x,1} + (\cos z_1)s_{y,1} \\ (-\sin z_2)s_{x,2} + (\cos z_2)s_{y,2} \\ \vdots \\ (-\sin z_I)s_{x,I} + (\cos z_I)s_{y,I} \end{bmatrix}$$

A weighted least squares solution uses bearing variances $\sigma_{\theta,i}^2$ through weights w_i:

$$w_i = \sigma_{\theta,i}^{-2}$$

Define

$$\mathbf{W} = \mathrm{diag}(w_1, w_2, \ldots, w_I)$$

Then the estimate is

$$\hat{\mathbf{x}} = (\mathbf{A}^T\mathbf{W}\mathbf{A})^{-1}\mathbf{A}^T\mathbf{W}\mathbf{b}$$

An approximate geolocation covariance for this linearized model is

$$\mathbf{P}_{\mathrm{LS}} \approx (\mathbf{A}^T\mathbf{W}\mathbf{A})^{-1}$$

This covariance directly supplies a TQ-style metric via trace($\mathbf{P}_{\mathrm{LS}}$) or its eigenvalues.

6.6. Target Confidence (TC) as Likelihood Accumulation

For CID, target confidence is commonly treated as a posterior probability that the observed emitter is consistent with a hypothesized target class or identity. Let the hypothesis be *H* (target-of-interest) versus $\bar{H}$ (not-of-interest). Let the bearing residual for node *i* relative to a predicted bearing $\theta_i^-(H)$ be

$$r_i = \mathrm{wrap}(z_i - \theta_i^-(H))$$

Assuming independent Gaussian bearing errors, the likelihood under *H* is

$$p(\mathbf{z} \mid H) = \prod_{i=1}^{I} \frac{1}{\sqrt{2\pi\sigma_{\theta,i}^2}} \exp\left(-\frac{r_i^2}{2\sigma_{\theta,i}^2}\right)$$

Similarly, define $p(\mathbf{z} \mid \bar{H})$ using a competing predicted bearing model or a clutter model.
The log-likelihood ratio is

$$\mathcal{L} = \log\frac{p(\mathbf{z} \mid H)}{p(\mathbf{z} \mid \bar{H})} = \sum_{i=1}^{I}\left[-\frac{r_i^2}{2\sigma_{\theta,i}^2} + \frac{\bar{r}_i^2}{2\bar{\sigma}_{\theta,i}^2}\right] + \mathrm{const}$$

A posterior target confidence is then

$$\mathrm{TC} = P(H \mid \mathbf{z}) = \frac{1}{1 + \exp\left(-(\mathcal{L} + \log\frac{P(H)}{P(\bar{H})})\right)}$$

where *P*(*H*) is the prior probability of the target-of-interest.
This formulation makes the role of DOA uncertainty explicit: smaller $\sigma_{\theta,i}^2$ increases the weight of residual consistency, increasing confidence when the geometry is consistent and reducing confidence when it is not.

6.7. How DOA-Derived Quantities Enter CID Scoring

The bearing estimate $\hat{\theta}$ enters as an observation *z*.

The bearing variance $\hat{\sigma}_\theta^2$ enters as the measurement noise term *R* or as weights $w_i = \sigma_{\theta,i}^{-2}$.

Track quality (TQ) is derived from posterior position covariance after bearing fusion, for example via trace($\mathbf{P}^+$) or trace($\mathbf{P}_{\mathrm{LS}}$).

Target confidence (TC) is derived from likelihood consistency of measured bearings with predicted bearings for a target hypothesis, explicitly weighted by $\sigma_{\theta,i}^2$.

In CID, subspace DOA provides a measurement model that directly constrains target position through bearing fusion, quantifies track quality through the resulting location covariance, and supports target confidence through likelihood-based consistency scoring in which the same DOA uncertainty terms determine the evidential weight of each observation.

7. Breakout for TQ

7.1. Track Quality (TQ) from Bearing-Only DOA Measurements

Track Quality (TQ) is treated here as a quantitative summary of track state uncertainty after fusing one or more DOA-derived bearing measurements. The core mathematical object is the posterior track covariance. A scalar TQ score is then derived from that covariance by a monotone mapping that penalizes large uncertainty and rewards concentrated uncertainty ellipses.

7.2. Track state and covariance

Use a planar kinematic track state at time step k:

$$\mathbf{x}_k = \begin{bmatrix} x_k \\ y_k \\ \dot{x}_k \\ \dot{y}_k \end{bmatrix}, \quad \mathbf{P}_k = \mathbb{E}\{(\mathbf{x}_k - \hat{\mathbf{x}}_k)(\mathbf{x}_k - \hat{\mathbf{x}}_k)^T\}$$

The measurement updates below can be used with an EKF. If only position is tracked, drop velocity terms and use the corresponding reduced matrices.

7.3. Bearing Measurement Model (Single Node)

Let the receiving node position at time k be:

$$\mathbf{s}_k = \begin{bmatrix} s_{x,k} \\ s_{y,k} \end{bmatrix}$$

A DOA estimator provides a bearing measurement:

$$z_k = \hat{\theta}_k$$

with variance:

$$R_k = \sigma_{\theta,k}^2$$

The nonlinear measurement function is:

$$h(\mathbf{x}_k) = \operatorname{atan2}(y_k - s_{y,k},\, x_k - s_{x,k})$$

Measurement equation:

$$z_k = h(\mathbf{x}_k) + v_k, \quad v_k \sim \mathcal{N}(0, R_k)$$

7.4. Jacobian

Define:

$$\Delta x_k = x_k - s_{x,k}, \quad \Delta y_k = y_k - s_{y,k}, \quad r_k^2 = \Delta x_k^2 + \Delta y_k^2$$

The Jacobian with respect to the full state is:

$$\mathbf{H}_k = \frac{\partial h}{\partial \mathbf{x}_k} = \begin{bmatrix} \frac{\partial h}{\partial x_k} & \frac{\partial h}{\partial y_k} & \frac{\partial h}{\partial \dot{x}_k} & \frac{\partial h}{\partial \dot{y}_k} \end{bmatrix} = \begin{bmatrix} -\frac{\Delta y_k}{r_k^2} & \frac{\Delta x_k}{r_k^2} & 0 & 0 \end{bmatrix}$$

7.5. EKF measurement update

Given a predicted (prior) track:

$$\hat{\mathbf{x}}_k^-, \quad \mathbf{P}_k^-$$

Innovation:

$$\tilde{y}_k = z_k - h(\hat{\mathbf{x}}_k^-)$$

Innovation covariance (scalar):

$$S_k = \mathbf{H}_k \mathbf{P}_k^- \mathbf{H}_k^T + R_k$$

Kalman gain:

$$\mathbf{K}_k = \mathbf{P}_k^- \mathbf{H}_k^T S_k^{-1}$$

State update:

$$\hat{\mathbf{x}}_k^+ = \hat{\mathbf{x}}_k^- + \mathbf{K}_k \tilde{y}_k$$

Covariance update:

$$\mathbf{P}_k^+ = (\mathbf{I} - \mathbf{K}_k \mathbf{H}_k)\mathbf{P}_k^-$$

Track Quality is derived from $\mathbf{P}_k^+$.

7.6. Position-Only Covariance Extracted from Full Covariance

Define the position covariance block:

$$\mathbf{P}_k^{xy} = \begin{bmatrix} P_{xx}^+ & P_{xy}^+ \\ P_{yx}^+ & P_{yy}^+ \end{bmatrix}$$

where these are the (1,1), (1,2), (2,1), (2,2) entries of $\mathbf{P}_k^+$.

7.7. Scalar Uncertainty Measures Used For TQ

A trace-based position error measure:

$$\mathrm{EPE}_k = \sqrt{\mathrm{trace}(\mathbf{P}_k^{xy})} = \sqrt{P_{xx}^+ + P_{yy}^+}$$

A determinant-based (area) measure:

$$\mathrm{AREA}_k = \sqrt{\det(\mathbf{P}_k^{xy})} = \sqrt{P_{xx}^+ P_{yy}^+ - (P_{xy}^+)^2}$$

Principal-axis measures via eigenvalues $\mu_{1,k} \geq \mu_{2,k}$ of $\mathbf{P}_k^{xy}$:

$$\mathbf{P}_k^{xy} \mathbf{q}_{i,k} = \mu_{i,k} \mathbf{q}_{i,k}$$

Ellipse semi-axis standard deviations:

$$\sigma_{1,k} = \sqrt{\mu_{1,k}}, \quad \sigma_{2,k} = \sqrt{\mu_{2,k}}$$

7.8. TQ Score as A Bounded Function of Covariance

A common bounded mapping uses an exponential penalty of uncertainty:
Trace-based TQ:

$$\mathrm{TQ}_k = \exp\left(-\frac{\mathrm{EPE}_k^2}{\tau^2}\right) = \exp\left(-\frac{P_{xx}^+ + P_{yy}^+}{\tau^2}\right)$$

Area-based TQ:

$$\mathrm{TQ}_k = \exp\left(-\frac{\mathrm{AREA}_k}{\alpha}\right) = \exp\left(-\frac{\sqrt{P_{xx}^+ P_{yy}^+ - (P_{xy}^+)^2}}{\alpha}\right)$$

Principal-axis based TQ (penalize worst axis):

$$\mathrm{TQ}_k = \exp\left(-\frac{\mu_{1,k}}{\beta}\right)$$

where tau, alpha, beta are application-chosen scale parameters that set the transition between “high” and “low” track quality.

7.9. Multi-Node Bearing Fusion and Its Effect On TQ

If multiple independent nodes provide bearings at the same update step, stack the measurements:

$$\mathbf{z}_k = \begin{bmatrix} z_{1,k} \\ z_{2,k} \\ \vdots \\ z_{I,k} \end{bmatrix}$$

Define the stacked measurement function:

$$\mathbf{h}(\mathbf{x}_k) = \begin{bmatrix} \operatorname{atan2}(y_k - s_{y,1,k},\, x_k - s_{x,1,k}) \\ \operatorname{atan2}(y_k - s_{y,2,k},\, x_k - s_{x,2,k}) \\ \vdots \\ \operatorname{atan2}(y_k - s_{y,I,k},\, x_k - s_{x,I,k}) \end{bmatrix}$$

The stacked Jacobian is:

$$\mathbf{H}_k = \begin{bmatrix} -\frac{\Delta y_{1,k}}{r_{1,k}^2} & \frac{\Delta x_{1,k}}{r_{1,k}^2} & 0 & 0 \\ -\frac{\Delta y_{2,k}}{r_{2,k}^2} & \frac{\Delta x_{2,k}}{r_{2,k}^2} & 0 & 0 \\ \vdots & \vdots & \vdots & \vdots \\ -\frac{\Delta y_{I,k}}{r_{I,k}^2} & \frac{\Delta x_{I,k}}{r_{I,k}^2} & 0 & 0 \end{bmatrix}$$

with:

$$\Delta x_{i,k} = x_k - s_{x,i,k}, \quad \Delta y_{i,k} = y_k - s_{y,i,k}, \quad r_{i,k}^2 = \Delta x_{i,k}^2 + \Delta y_{i,k}^2$$

Measurement noise covariance (diagonal if independent):

$$\mathbf{R}_k = \mathrm{diag}(\sigma^2_{\theta,1,k}, \ldots, \sigma^2_{\theta,I,k})$$

Then:

$$\mathbf{S}_k = \mathbf{H}_k \mathbf{P}_k^- \mathbf{H}_k^T + \mathbf{R}_k$$

$$\mathbf{K}_k = \mathbf{P}_k^- \mathbf{H}_k^T \mathbf{S}_k^{-1}$$

$$\hat{\mathbf{x}}_k^+ = \hat{\mathbf{x}}_k^- + \mathbf{K}_k(\mathbf{z}_k - \mathbf{h}(\hat{\mathbf{x}}_k^-))$$

$$\mathbf{P}_k^+ = (\mathbf{I} - \mathbf{K}_k \mathbf{H}_k)\mathbf{P}_k^-$$

As I increases or $\sigma^2_{\theta,i,k}$ decreases, $\mathbf{P}_k^+$ contracts and TQ increases by construction.

7.10. TQ Contribution from Pseudospectrum-Derived Bearing Variance

The DOA estimator supplies $\sigma^2_{\theta,k}$ (or a proxy). In the EKF update, this enters directly as:

$$R_k = \sigma^2_{\theta,k}$$

Smaller R_k produces smaller innovation covariance S_k, larger gain in informative directions, and a stronger reduction in $\mathbf{P}_k^+$ increasing TQ. Larger R_k produces weaker covariance contraction, decreasing TQ.

Track Quality is a deterministic function of posterior track covariance after bearing fusion. Subspace DOA enters the track filter through the bearing observation z and its uncertainty $R = \sigma_\theta^2$, which govern how strongly each update contracts the uncertainty ellipse. A scalar TQ score is then formed by mapping a covariance-derived uncertainty measure such as trace, determinant, or principal-axis eigenvalue into a bounded confidence score.

8. Array Configuration

Consider an array of M spatially separated sensors (antennas). Assume the array is illuminated by K narrowband plane waves arriving from distinct directions

$$\{\theta_1, \theta_2, \ldots, \theta_K\}$$

with the constraint

$$K < M$$

This constraint is required so that the array has enough spatial degrees of freedom to resolve multiple sources.

8.1. Narrowband Plane-Wave Model

Assume that each source signal is narrowband relative to the propagation delay across the array aperture. Under this assumption, time delays between sensors can be represented as phase shifts, and the received signal at the array can be modeled using steering vectors.

Let $\mathbf{x}(n) \in \mathbb{C}^M$ denote the complex baseband snapshot vector at discrete time index n where each element corresponds to the sampled IQ value from one antenna.

8.2. Snapshot Equation

The received snapshot is modeled as the superposition of k sources plus additive noise:

$$\mathbf{x}(n) = \sum_{k=1}^{K} \mathbf{a}(\theta_k) s_k(n) + \mathbf{w}(n)$$

where:
$\mathbf{a}(\theta_k) \in \mathbb{C}^M$ is the steering vector associated with a plane wave arriving from direction θ_k
$s_k(n) \in \mathbb{C}$ is the complex source waveform at snapshot n
$\mathbf{w}(n) \in \mathbb{C}^M$ is additive noise

8.3. Noise Assumptions

The noise vector is commonly modeled as spatially white, temporally uncorrelated, circular complex Gaussian noise:

$$\mathbf{w}(n) \sim \mathcal{CN}(\mathbf{0}, \sigma^2 \mathbf{I})$$

where σ^2 is the noise variance and $\mathbf{I}$ is the $M \times M$ identity matrix.

8.4. Matrix Form

Define the steering matrix

$$\mathbf{A} = \begin{bmatrix} \mathbf{a}(\theta_1) & \mathbf{a}(\theta_2) & \cdots & \mathbf{a}(\theta_K) \end{bmatrix} \in \mathbb{C}^{M \times K}$$

and the source vector

$$\mathbf{s}(n) = \begin{bmatrix} s_1(n) \\ s_2(n) \\ \vdots \\ s_K(n) \end{bmatrix} \in \mathbb{C}^K$$

Then the snapshot equation can be written compactly as

$$\mathbf{x}(n) = \mathbf{A}\mathbf{s}(n) + \mathbf{w}(n)$$

This representation separates deterministic spatial structure (contained in **A**) from unknown source amplitudes (contained in s(n)). MUSIC exploits this structure by estimating the subspace spanned by the columns of **A** through the eigenstructure of the spatial covariance matrix.

8.5. Notes

The MUSIC problem begins with a narrowband linear array model in which each source direction induces a distinct steering vector. The observed array snapshot is a linear combination of these steering vectors weighted by unknown source waveforms, corrupted by additive noise. The unknown parameters of interest are the arrival angles $\theta_1, \ldots, \theta_K$, which are inferred indirectly through covariance structure and subspace orthogonality.

9. Spatial Covariance Matrix

The spatial covariance matrix captures the second-order statistical structure of the signals received by the antenna array. It is the central object in subspace-based direction-of-arrival estimation methods such as MUSIC, as its eigenstructure encodes the separation between signal and noise components.

9.1. Definition

Let $\mathbf{x}(n) \in \mathbb{C}^M$ denote the array snapshot at time index n. The spatial covariance matrix $\mathbf{R} \in \mathbb{C}^{M \times M}$ is defined as the expected outer product of the snapshot with its Hermitian transpose:

$$\mathbf{R} = \mathbb{E}\{\mathbf{x}(n)\mathbf{x}^H(n)\}$$

This matrix summarizes average spatial correlations between all sensor pairs.

9.2. Substitution of The Signal Model

Substituting the array signal model

$$\mathbf{x}(n) = \mathbf{A}\mathbf{s}(n) + \mathbf{w}(n)$$

into the covariance definition yields:

$$\mathbf{R} = \mathbb{E}\{(\mathbf{A}\mathbf{s} + \mathbf{w})(\mathbf{A}\mathbf{s} + \mathbf{w})^H\}$$

Expanding the expectation gives:

$$\mathbf{R} = \mathbf{A}\mathbb{E}\{\mathbf{s}\mathbf{s}^H\}\mathbf{A}^H + \mathbb{E}\{\mathbf{w}\mathbf{w}^H\} + \mathbf{A}\mathbb{E}\{\mathbf{s}\mathbf{w}^H\} + \mathbb{E}\{\mathbf{w}\mathbf{s}^H\}\mathbf{A}^H$$

Assuming the source signals and noise are uncorrelated,

$$\mathbb{E}\{\mathbf{s}\mathbf{w}^H\} = \mathbf{0}$$

and assuming spatially white noise with variance σ^2 ,

$$\mathbb{E}\{\mathbf{w}\mathbf{w}^H\} = \sigma^2\mathbf{I}$$

the covariance matrix simplifies to:

$$\mathbf{R} = \mathbf{A}\mathbf{R}_s\mathbf{A}^H + \sigma^2\mathbf{I}$$

where

is the $K \times K$ source covariance matrix.

9.3. Structure and Interpretation

The term $\mathbf{A}\mathbf{R}_s\mathbf{A}^H$ has rank at most K and spans the signal subspace of the array measurements. The additive term $\sigma^2\mathbf{I}$ represents isotropic noise that uniformly elevates all eigenvalues without altering eigenvectors.

This additive structure is what enables separation of signal and noise subspaces via eigenvalue decomposition.

9.4. Sample Covariance Estimate

In practice, the ensemble expectation $\mathbb{E}\{\cdot\}$ is unknown and must be approximated using a finite number of snapshots.
Given N independent snapshots $\mathbf{x}(1),\ldots, \mathbf{x}(N)$, the sample covariance matrix is defined as:

$$\hat{\mathbf{R}} = \frac{1}{N}\sum_{n=1}^{N}\mathbf{x}(n)\mathbf{x}^H(n)$$

This estimator is Hermitian and positive semidefinite by construction.

9.5. Asymptotic Behavior

As the number of snapshots N increases,

$$\hat{\mathbf{R}} \to \mathbf{R}$$

in the mean-square sense, provided the snapshots are independent and identically distributed. In finite-sample regimes, estimation error perturbs the eigenvalues and eigenvectors, which directly impacts MUSIC performance.

9.6. Role in MUSIC

The spatial covariance matrix is the sole input to the eigenstructure-based decomposition used by MUSIC. Its eigenvectors define the signal and noise subspaces, and its eigenvalue separation governs the resolution and robustness of direction estimates.

9.7. Notes

The spatial covariance matrix encodes the second-order spatial statistics of array measurements. Under standard assumptions, it decomposes into a low-rank signal component and an isotropic noise component. MUSIC exploits this structure by identifying steering vectors that are orthogonal to the noise subspace derived from the covariance matrix.

9.8. Eigenvalue Decomposition of The Covariance Matrix

Let $\mathbf{R} \in \mathbb{C}^{M\times M}$ denote the spatial covariance matrix. Its eigenvalue decomposition is given by

$$\mathbf{R} = \mathbf{U}\boldsymbol{\Lambda}\mathbf{U}^{H}$$

where:
$\mathbf{U} = [\mathbf{u}_1, \mathbf{u}_2,\ldots, \mathbf{u}_M]$ is a unitary matrix whose columns are the eigenvectors of $\mathbf{R}$
$\boldsymbol{\Lambda} = \mathrm{diag}(\lambda_1, \lambda_2,\ldots, \lambda_M)$ is a diagonal matrix of real, nonnegative eigenvalues

The eigenvectors satisfy orthonormality:

$$\mathbf{U}^{H}\mathbf{U} = \mathbf{U}\mathbf{U}^{H} = \mathbf{I}$$

9.9. Eigenvalue Ordering and Interpretation

Under the standard array signal model with K uncorrelated sources and spatially white noise, the eigenvalues of $\mathbf{R}$ satisfy

$$\lambda_1 \geq \lambda_2 \geq \cdots \geq \lambda_K > \lambda_{K+1} = \cdots = \lambda_M = \sigma^2$$

The largest K eigenvalues correspond to signal energy projected onto the array, while the remaining $M - K$ eigenvalues correspond to noise power.

The separation between these two sets of eigenvalues reflects the signal-to-noise ratio and determines how clearly the signal and noise subspaces can be distinguished.

9.10. Subspace Partitioning

The eigenvectors associated with the largest K eigenvalues span the signal subspace:

$$\mathbf{U}_s = \begin{bmatrix}\mathbf{u}_1 & \mathbf{u}_2 & \ldots & \mathbf{u}_K\end{bmatrix} \in \mathbb{C}^{M\times K}$$

This subspace contains all steering vectors corresponding to the true directions of arrival.
The eigenvectors associated with the remaining $M - K$ eigenvalues span the noise subspace:

$$\mathbf{U}_n = \begin{bmatrix}\mathbf{u}_{K+1} & \mathbf{u}_{K+2} & \ldots & \mathbf{u}_M\end{bmatrix} \in \mathbb{C}^{M\times(M-K)}$$

This subspace is orthogonal to the signal subspace by construction.

9.11. Orthogonality Property

Because $\mathbf{U}$ is unitary, the signal and noise subspaces satisfy

$$\mathbf{U}_s^{H}\mathbf{U}_n = \mathbf{0}$$

This orthogonality underlies the MUSIC algorithm: steering vectors corresponding to true source directions lie in the signal subspace and therefore have zero projection onto the noise subspace.

9.12. Practical Considerations

In finite-sample conditions, the equality $\lambda_{K+1} = \cdots = \lambda_M = \sigma^2$ is only approximate. Noise eigenvalues form a cluster rather than a perfect plateau, and eigenvalue spread increases as snapshot count decreases or SNR degrades.

Estimating the number of sources K typically relies on eigenvalue gap inspection or information-theoretic criteria such as AIC or MDL.

9.13. Role in MUSIC

The eigenvalue decomposition transforms the covariance matrix into a basis where signal and noise components are explicitly separated. MUSIC uses the noise-subspace eigenvectors to construct a pseudospectrum whose peaks identify directions of arrival with resolution beyond classical beamforming limits.

9.14. Notes

Eigenvalue decomposition of the spatial covariance matrix partitions the measurement space into orthogonal signal and noise subspaces. This partitioning enables MUSIC to detect directions of arrival by identifying steering vectors that are orthogonal to the noise subspace, with performance governed by eigenvalue separation and estimation accuracy.

10. Subspace Orthogonality Principle

The defining theoretical property exploited by the MUSIC algorithm is the orthogonality between the signal and noise subspaces of the spatial covariance matrix. This property provides the mathematical basis for identifying directions of arrival through subspace projection.

10.1. Steering vectors and the signal subspace

Under the array signal model, the steering vectors associated with true source directions span the same subspace as the columns of the steering matrix $\mathbf{A}$. Because the signal subspace $\mathbf{U}_s$ is defined as the eigenspace corresponding to the K largest eigenvalues of the covariance matrix, it follows that each steering vector corresponding to a true source direction lies entirely within this subspace:

$$\mathbf{a}(\theta_k) \in \text{span}(\mathbf{U}_s), \quad k = 1, \ldots, K$$

Equivalently, each steering vector can be expressed as a linear combination of the signal-subspace eigenvectors:

$$\mathbf{a}(\theta_k) = \mathbf{U}_s \mathbf{c}_k$$

for some coefficient vector $\mathbf{c}_k \in \mathbb{C}^K$.

10.2. Orthogonality to The Noise Subspace

Because the full eigenvector matrix $\mathbf{U}$ is unitary, the signal and noise subspaces are orthogonal complements of one another. This implies that any vector lying in the signal subspace must be orthogonal to all vectors spanning the noise subspace:

$$\mathbf{U}_n^H \mathbf{a}(\theta_k) = \mathbf{0}$$

This condition holds exactly in the idealized case of infinite snapshots, spatially white noise, and perfectly known array geometry. In practical scenarios, the equality is approximate rather than exact.

10.3. Geometric Interpretation

Geometrically, MUSIC searches for steering vectors that lie in the null space of the noise subspace projector. For a hypothesized direction θ that matches a true source direction, the corresponding steering vector has no component in the noise subspace. For incorrect directions, the steering vector has a nonzero projection onto the noise subspace.

10.4. Role in Pseudospectrum Construction

The MUSIC pseudospectrum is constructed by measuring the energy of the projection of each steering vector onto the noise subspace. Directions for which this projection energy is minimal correspond to candidate directions of arrival. The sharpness of these minima is

responsible for the high-resolution properties of MUSIC.

10.5. Notes

The subspace orthogonality principle states that steering vectors corresponding to true source directions lie entirely within the signal subspace and are orthogonal to the noise subspace. MUSIC exploits this property by identifying directions whose steering vectors minimize projection onto the noise subspace, forming the mathematical foundation of the algorithm.

11. MUSIC Pseudospectrum

The MUSIC (Multiple Signal Classification) algorithm estimates directions of arrival by exploiting the structure of the spatial covariance matrix of an antenna array. Rather than forming beams and measuring output power, MUSIC evaluates how well a hypothesized steering vector aligns with the signal subspace of the received data. Directions that are consistent with the observed signal subspace correspond to minima in the projection onto the noise subspace, which appear as sharp peaks in a constructed pseudospectrum.

The method relies on the separation of signal and noise subspaces induced by the eigenstructure of the covariance matrix. This separation enables resolution beyond classical beamforming limits when the underlying assumptions are satisfied.

11.1. Array Signal Model

Consider an array of M sensors receiving K narrowband plane waves, with $K < M$. The received complex baseband signal at snapshot n is modeled as

$$\mathbf{x}(n) = \sum_{k=1}^{K} \mathbf{a}(\theta_k) s_k(n) + \mathbf{w}(n)$$

where $\mathbf{x}(n) \in \mathbb{C}^M$ is the array snapshot, $\mathbf{a}(\theta_k) \in \mathbb{C}^M$ is the steering vector corresponding to direction θ_k, $s_k(n)$ is the source signal, and $\mathbf{w}(n)$ is additive noise, assumed spatially white with variance σ^2.

In matrix form,

$$\mathbf{x}(n) = \mathbf{A}\mathbf{s}(n) + \mathbf{w}(n)$$

with $\mathbf{A} = [\mathbf{a}(\theta_1) \ldots \mathbf{a}(\theta_K)]$.

11.2. Spatial Covariance Matrix

The spatial covariance matrix is defined as

$$\mathbf{R} = \mathbb{E}\{\mathbf{x}\mathbf{x}^H\}$$

Substituting the signal model yields

$$\mathbf{R} = \mathbf{A}\mathbf{R}_s\mathbf{A}^H + \sigma^2\mathbf{I}$$

where $\mathbf{R}_s = \mathbb{E}\{\mathbf{s}\mathbf{s}^H\}$ is the source covariance matrix and $\mathbf{I}$ is the identity matrix. In practice, $\mathbf{R}$ is estimated from a finite number of snapshots.

11.3. Orthogonality Principle

For each true source direction θ_k, the steering vector $\mathbf{a}(\theta_k)$ lies in the column space of $\mathbf{A}$ and therefore in the signal subspace. Consequently, it is orthogonal to the noise subspace:

$$\mathbf{U}_n^H \mathbf{a}(\theta_k) = \mathbf{0}$$

This orthogonality condition is exact in the idealized case of infinite data, uncorrelated sources, and spatially white noise, and approximate in practical scenarios.

11.4. Noise-Subspace Projection

Define the projection of a steering vector onto the noise subspace as

$$\mathbf{y}(\theta) = \mathbf{U}_n^H \mathbf{a}(\theta)$$

The squared norm of this projection is

$$\|\mathbf{y}(\theta)\|_2^2 = \mathbf{a}^H(\theta)\mathbf{U}_n\mathbf{U}_n^H\mathbf{a}(\theta)$$

This quantity measures the degree to which the hypothesized steering vector is inconsistent with the signal subspace implied by the data.

11.5. Interpretation

The MUSIC pseudospectrum is not a power spectrum. Instead, it is an inverse consistency metric that highlights directions whose steering vectors align with the signal subspace extracted from the covariance matrix. Its high resolution arises from subspace separation rather than aperture-limited beamforming, with performance governed by signal-to-noise ratio, snapshot count, array calibration accuracy, and source separability.

11.6. Notes

MUSIC constructs a pseudospectrum by projecting hypothesized steering vectors onto the noise subspace of the array covariance matrix. Directions of arrival are identified as those that minimize this projection, corresponding to maxima of the reciprocal projection energy. The mathematical core of the method is the eigenstructure-based decomposition of the covariance matrix and the resulting orthogonality between steering vectors and the noise subspace.

12. Steering Vector for a Uniform Linear Array

A steering vector encodes the relative phase response across an antenna array for a plane wave arriving from a given direction. In MUSIC and related array-processing methods, the steering vector represents the deterministic spatial signature of a hypothesized source direction and is the fundamental object tested against the signal and noise subspaces.

12.1. Array Geometry and Assumptions

Consider a uniform linear array (ULA) consisting of M identical antenna elements arranged along a straight line with equal inter-element spacing d. The array is assumed to be:

• Narrowband, so that phase differences across the array can be modeled as constant phase shifts
• In the far field of the source, so that incoming wavefronts are planar
• Calibrated, with identical element responses

Let θ denote the angle of arrival measured relative to array broadside (normal to the array axis).

12.2. Plane-Wave Phase Model

A monochromatic plane wave with wavelength λ arriving at angle θ has a propagation vector whose projection along the array axis introduces a path-length difference between adjacent elements of:

$$\Delta\ell = d\sin\theta$$

This path difference corresponds to a phase shift:

$$\Delta\phi = \frac{2\pi}{\lambda} d\sin\theta$$

Between successive antenna elements, the received signal accumulates an additional phase of $-\Delta\phi$.

12.3. Steering Vector Definition

The steering vector $\mathbf{a}(\theta) \in \mathbb{C}^M$ is defined as the collection of relative phase responses across the array, normalized with respect to the first element:

$$\mathbf{a}(\theta) = \begin{bmatrix} 1 \\ e^{-j\frac{2\pi}{\lambda}d\sin\theta} \\ e^{-j\frac{2\pi}{\lambda}2d\sin\theta} \\ \vdots \\ e^{-j\frac{2\pi}{\lambda}(M-1)d\sin\theta} \end{bmatrix}$$

Equivalently, the m-th element of the steering vector can be written explicitly as:

$$a_m(\theta) = e^{-j\frac{2\pi}{\lambda}(m-1)d\sin\theta}, \quad m = 1, \ldots, M$$

12.4. Compact Exponential Form

Defining the spatial frequency

$$k = \frac{2\pi}{\lambda}$$

the steering vector becomes:

$$\mathbf{a}(\theta) = \begin{bmatrix} e^{-jk(0)d\sin\theta} \\ e^{-jk(1)d\sin\theta} \\ \vdots \\ e^{-jk(M-1)d\sin\theta} \end{bmatrix}$$

This form highlights that the steering vector is a sampled complex exponential across the array aperture.

12.5. Interpretation in MUSIC

In the MUSIC algorithm, $\mathbf{a}(\theta)$ represents the expected spatial signature of a source arriving from direction θ. The pseudospectrum evaluates how orthogonal this vector is to the estimated noise subspace:

• If θ matches a true source direction, $\mathbf{a}(\theta)$ lies in the signal subspace
• If θ does not correspond to a source, $\mathbf{a}(\theta)$ has a significant projection onto the noise subspace

The sharpness of MUSIC peaks depends on how accurately the steering vector models the true array geometry and wavelength.

12.6. Practical Considerations

The inter-element spacing is typically chosen as:

$$d \leq \frac{\lambda}{2}$$

to avoid spatial aliasing (grating lobes). Calibration errors, mutual coupling, and element position uncertainty distort the steering vector and directly degrade MUSIC performance.

12.7. Notes

For a uniform linear array, the steering vector is a deterministic complex exponential whose phase progression is governed by array spacing, wavelength, and arrival angle. In subspace-based DOA estimation, it serves as the hypothesis tested against the noise subspace to identify directions of arrival with super-resolution accuracy.

13. Algorithmic Procedure

Compute $\hat{\mathbf{R}}$ from array snapshots.

Perform eigenvalue decomposition of $\hat{\mathbf{R}}$.

Estimate K using eigenvalue thresholding or information criteria (AIC/MDL).

Form the noise subspace $\mathbf{U}_n$.

Evaluate $P_{\text{MUSIC}}(\theta)$ over a search grid.

Locate peaks corresponding to estimated directions of arrival.

13.1. Key Assumptions

Signals are narrowband relative to array aperture.

Sources are uncorrelated.

Noise is spatially white.

Array geometry is known and calibrated.

Number of sensors exceeds number of sources.

14. Master equation

The preceding derivations are now collected into an explicit form suitable for implementation.

14.1. Input Data and Indexing

Let the array have M antenna elements. Let there be N complex baseband snapshots. The raw complex sample from antenna m at snapshot n is

$$x_m(n) \in \mathbb{C}, \qquad m \in \{1, \ldots, M\}, \qquad n \in \{1, \ldots, N\}.$$

Define the snapshot vector (column)

$$\mathbf{x}(n) = \begin{bmatrix} x_1(n) \\ x_2(n) \\ \vdots \\ x_M(n) \end{bmatrix} \in \mathbb{C}^{M \times 1}.$$

If code uses zero-based indices, map $m_{\text{code}} = m - 1$ and $n_{\text{code}} = n - 1$, but keep the algebra below unchanged.

14.2. Mean Removal Used by The Covariance Estimator

MUSIC derivations typically assume the snapshot vector is mean-zero in time. If the data are not mean-zero, remove the sample mean per channel before forming the covariance.

Sample mean per antenna:

$$\hat{\mu}_m = \frac{1}{N} \sum_{n=1}^{N} x_m(n), \qquad m \in \{1, \ldots, M\}.$$

Mean-removed samples:

$$\tilde{x}_m(n) = x_m(n) - \hat{\mu}_m.$$

If mean removal is used, replace $x_m(n)$ by $\tilde{x}_m(n)$ everywhere in the covariance sums below.

14.3. Sample Covariance Matrix Entries

The sample covariance matrix $\hat{\mathbf{R}} \in \mathbb{C}^{M \times M}$ is defined entry-wise as

$$\hat{R}_{ij} = \frac{1}{N} \sum_{n=1}^{N} x_i(n)\, x_j^*(n), \qquad i, j \in \{1, \dots, M\}.$$

Equivalently, in terms of snapshot-vector components,

$$\hat{R}_{ij} = \frac{1}{N} \sum_{n=1}^{N} [\mathbf{x}(n)]_i \; [\mathbf{x}(n)]_j^* \, .$$

Hermitian structure follows directly from the definition:

$\hat{R}_{ji} = \hat{R}_{ij}^*$. Diagonal entries are nonnegative reals:

$$\hat{R}_{ii} = \frac{1}{N} \sum_{n=1}^{N} |x_i(n)|^2 \in \mathbb{R}_{\geq 0}.$$

14.4. Complex Product Expanded into Real and Imaginary Parts

If an implementation stores complex samples as $(\Re, \Im)$ pairs, write

$$x_i(n) = a_i(n) + j\, b_i(n), \qquad x_j(n) = a_j(n) + j\, b_j(n),$$

so

$$x_j^*(n) = a_j(n) - j\, b_j(n).$$

Then the covariance summand expands as

$$x_i(n)\, x_j^*(n) = \big(a_i(n) a_j(n) + b_i(n) b_j(n)\big) + j\, \big(b_i(n) a_j(n) - a_i(n) b_j(n)\big) \, .$$

Therefore the real and imaginary parts of $\hat{R}_{ij}$ are

$$\Re\{\hat{R}_{ij}\} = \frac{1}{N} \sum_{n=1}^{N} \Big(a_i(n) a_j(n) + b_i(n) b_j(n)\Big),$$

$$\Im\{\hat{R}_{ij}\} = \frac{1}{N} \sum_{n=1}^{N} \Big(b_i(n) a_j(n) - a_i(n) b_j(n)\Big).$$

15. Eigenstructure Extraction

Because $\hat{\mathbf{R}}$ is Hermitian, it has M real eigenvalues and an orthonormal eigenvector basis. Compute eigenpairs $(\hat{\lambda}_\ell, \hat{\mathbf{u}}_\ell)$ such that

$$\hat{\mathbf{R}}\hat{\mathbf{u}}_\ell = \hat{\lambda}_\ell \hat{\mathbf{u}}_\ell, \qquad \ell \in \{1, \ldots, M\}.$$

Write eigenvector ℓ in components as

$$\hat{\mathbf{u}}_\ell = \begin{bmatrix} \hat{u}_{1,\ell} \\ \hat{u}_{2,\ell} \\ \vdots \\ \hat{u}_{M,\ell} \end{bmatrix}.$$

Then the eigenvalue equation is, for every row index i,

$$\sum_{j=1}^{M} \hat{R}_{ij}\, \hat{u}_{j,\ell} = \hat{\lambda}_\ell\, \hat{u}_{i,\ell}, \qquad i \in \{1, \ldots, M\}, \qquad \ell \in \{1, \ldots, M\}.$$

15.1. Orthonormality Constraints in Summation Notation

Hermitian EVD yields orthonormal eigenvectors:

$$\sum_{m=1}^{M} \hat{u}^*_{m,\ell} \hat{u}_{m,\ell'} = \delta_{\ell,\ell'}, \qquad \ell, \ell' \in \{1, \ldots, M\}.$$

where $\delta_{\ell,\ell'} = 1$ if $\ell = \ell'$ and 0 otherwise.

15.2. Eigenvalue Sorting and The Noise-Subspace Index Mapping

Sort eigenvalues in descending order:

$$\hat{\lambda}_1 \geq \hat{\lambda}_2 \geq \cdots \geq \hat{\lambda}_M.$$

Let $\hat{K}$ be the chosen model order (number of sources). Then the noise subspace uses the eigenvectors associated with the smallest $(M - \hat{K})$ eigenvalues, i.e. eigenvector indices $\ell = \hat{K} + 1, \ldots, M$.

Define a noise-mode column index $r \in \{1, \ldots, M - \hat{K}\}$ mapped to eigenvector index $\ell = \hat{K} + r$. Define

$$u_{m,r} \triangleq \hat{u}_{m,\hat{K}+r}, \qquad m \in \{1, \ldots, M\}, \qquad r \in \{1, \ldots, M - \hat{K}\}.$$

The noise-subspace eigenvector matrix $\mathbf{U}_n \in \mathbb{C}^{M \times (M-\hat{K})}$ has entries $u_{m,r}$ by construction.

16. Noise-Subspace Projection and The MUSIC Denominator

16.1. Steering Vector Component Definition

For each scan angle $\theta \in \Theta$, define a steering vector

$$\mathbf{a}(\theta) = \begin{bmatrix} a_1(\theta) \\ a_2(\theta) \\ \vdots \\ a_M(\theta) \end{bmatrix} \in \mathbb{C}^{M\times 1}.$$

No normalization is assumed unless explicitly inserted. If a unit-norm steering vector is required, define

$$\tilde{a}_m(\theta) = \frac{a_m(\theta)}{\sqrt{\sum_{q=1}^{M} |a_q(\theta)|^2}},$$

and substitute $\tilde{a}_m(\theta)$ for $a_m(\theta)$ in all sums below.

16.2. Noise-Subspace Projection Coefficients Written as Explicit Inner Products

For each noise mode r, define the scalar projection coefficient

$$y_r(\theta) = \sum_{m=1}^{M} u_{m,r}^{*}\, a_m(\theta), \qquad r \in \{1, \ldots, M - \hat{K}\}.$$

Its complex conjugate is

$$y_r^{*}(\theta) = \left(\sum_{m=1}^{M} u_{m,r}^{*}\, a_m(\theta) \right)^{*} = \sum_{p=1}^{M} u_{p,r}\, a_p^{*}(\theta).$$

16.3. Denominator Energy as A Sum of Squared Magnitudes

Define the MUSIC denominator (noise-projection energy) as

$$d(\theta) = \sum_{r=1}^{M-\hat{K}} |y_r(\theta)|^2 = \sum_{r=1}^{M-\hat{K}} y_r(\theta)\, y_r^{*}(\theta).$$

Substitute the explicit sums for $y_r(\theta)$ and $y_r^{*}(\theta)$:

$$d(\theta) = \sum_{r=1}^{M-\hat{K}} \left(\sum_{m=1}^{M} u_{m,r}^{*}\, a_m(\theta) \right) \left(\sum_{p=1}^{M} u_{p,r}\, a_p^{*}(\theta) \right).$$

Expand the product into a triple sum:

$$d(\theta) = \sum_{r=1}^{M-\hat{K}} \sum_{m=1}^{M} \sum_{p=1}^{M} u_{m,r}^{*}\, u_{p,r}\, a_m(\theta)\, a_p^{*}(\theta).$$

16.4. Real-Valuedness And Numerical Enforcement

In exact arithmetic, $d(\theta) \geq 0$ and $d(\theta) \in \mathbb{R}$. In finite precision, a small imaginary residue can appear. Enforce real-valuedness by

$$d_{\text{real}}(\theta) = \frac{d(\theta) + d^{*}(\theta)}{2} = \Re\{d(\theta)\}.$$

Use $d_{\text{real}}(\theta)$ in the denominator if this enforcement is applied.

16.5. Pseudospectrum Definition

Define the MUSIC pseudospectrum as

$$P_{\text{MUSIC}}(\theta) = \frac{1}{d(\theta)}.$$

This is equivalent to the projector form

$P_{\text{MUSIC}}(\theta) = 1/\left(\mathbf{a}^H(\theta)\mathbf{U}_n\mathbf{U}_n^H\mathbf{a}(\theta)\right)$ but written entirely as explicit sums.

16.6. Pseudospectrum With A Numerical Floor

For implementation stability, apply a floor $\epsilon > 0$:

$$P_{\text{MUSIC}}(\theta) = \left[\max\left(d(\theta), \epsilon\right)\right]^{-1}.$$

If real-valued enforcement is used, replace $d(\theta)$ by $d_{\text{real}}(\theta)$ in the max(·).

16.7. ULA Steering Vector Component

Assume a uniform linear array with inter-element spacing d, wavelength λ, and a broadside-referenced angle θ such that phase progression is proportional to sin θ. Let element positions be $d_m = (m-1)d$. A standard steering vector form is

$$a_m(\theta) = \exp\left(-j\frac{2\pi}{\lambda}(m-1)d\sin\theta\right), \qquad m \in \{1, \ldots, M\}.$$

The conjugate component is

$$a_p^*(\theta) = \exp\left(+j\frac{2\pi}{\lambda}(p-1)d\sin\theta\right), \qquad p \in \{1, \ldots, M\}.$$

16.8. Denominator with ULA substitution

Insert the ULA $a_m(\theta)$ and $a_p^*(\theta)$ into the triple sum for $d(\theta)$:

$$d(\theta) = \sum_{r=1}^{M-\hat{K}} \sum_{m=1}^{M} \sum_{p=1}^{M} u_{m,r}^* \, u_{p,r} \, \exp\left(-j\frac{2\pi}{\lambda}(m-1)d\sin\theta\right) \exp\left(+j\frac{2\pi}{\lambda}(p-1)d\sin\theta\right).$$

No algebraic collapsing is applied. This is a direct substitution in nested-sum form.

16.9. Master Equation for $P_{\text{MUSIC}}(\theta)$ with ULA Substitution

Combine the floor and reciprocal:

$$P_{\text{MUSIC}}(\theta) = \left[\max\left(\sum_{r=1}^{M-\hat{K}} \sum_{m=1}^{M} \sum_{p=1}^{M} u_{m,r}^* \, u_{p,r} \, \exp\left(-j\frac{2\pi}{\lambda}(m-1)d\sin\theta\right) \exp\left(+j\frac{2\pi}{\lambda}(p-1)d\sin\theta\right), \epsilon\right)\right]^{-1}.$$

This is the end-to-end evaluation equation once $\{u_{m,r}\}$ have been computed from the eigendecomposition of $\hat{\mathbf{R}}$.

17. Scan-Grid Evaluation Written as Explicit Discrete Equations

17.1. Discrete Scan Grid Definition

Let the scan grid be the finite set

$$\Theta = \{\theta_1, \theta_2, \ldots, \theta_Q\}.$$

Compute the pseudospectrum sample for each grid point:

$$P_q \triangleq P_{\text{MUSIC}}(\theta_q), \qquad q \in \{1, \ldots, Q\}.$$

17.2. Peak Selection Without Abstraction

A single DOA estimate (single peak) is

$$\hat{\theta} = \theta_{\hat{q}}, \qquad \hat{q} = \arg \max_{q \in \{1,\ldots,Q\}} P_q.$$

For multiple sources, identify the $\hat{K}$ largest local maxima of $\{P_q\}$ subject to a separation rule consistent with grid resolution and expected source spacing.

18. Adding in Atmospherics

Our lab characterizes atmospheric propagation using atmospheric probe lasers that measure refractive and absorptive behavior over a range of frequencies. These frequency-dependent effects are reduced into compact recursive polynomial parameterizations that can be evaluated efficiently inside the propagation model. The resulting ray formulation is treated as a geometric-optics approximation, with propagation solved at a single narrowband carrier frequency ω_0 per MUSIC evaluation. Reflection and refraction effects are included through the refractive-index field and associated ray bending, while multipath is either neglected or absorbed into a stochastic residual error term. The atmosphere is assumed quasi-static over the snapshot window used to form $\hat{\mathbf{R}}$, so that the ray-integrated phase and attenuation are treated as deterministic during the covariance accumulation interval [6,7].

The MUSIC workflow evaluates a quadratic form of the type

$y_r(\theta) = \sum_{m=1}^{M} u_{m,r}^{*} a_m(\theta)$ and then accumulates

$d(\theta) = \sum_r |y_r(\theta)|^2$. In an analytic ray-tracing context, the same structure is obtained when the per-sensor complex field is written as a path integral that includes deterministic phase, deterministic attenuation, and random phase/ amplitude error. The ray tracer provides $a_m(\theta)$ by propagating a candidate direction through a refracting and lossy medium to each sensor location, then returning the complex field at the receiver.

18.1. Geometry and State Variables

Let $\mathbf{s}_m \in \mathbb{R}^3$ be the position of sensor m, and let a candidate direction be parameterized by angle θ (or a unit direction vector $\hat{\mathbf{u}}(\theta) \in \mathbb{R}^3$). Let the ray path for sensor m be $\mathbf{r}_m(\ell; \theta)$, parameterized by arc length $\ell \in [0, L_m(\theta)]$, with tangent $\hat{\mathbf{t}}_m(\ell; \theta) = d\mathbf{r}_m$.

Assume a carrier angular frequency ω_0 and free-space wavenumber $k_0 = \omega_0/c$, where c is the vacuum speed of light. Let the refractive index be $n(\mathbf{r}, t) = 1 + \Delta n(\mathbf{r}, t)$ with $|\Delta n| \ll 1$. Let the specific attenuation along the path be $\alpha(\mathbf{r}, t)$ in nepers per meter. Let $G_m(\theta)$ represent calibrated element pattern and receiver complex gain (dimensionless).

18.2. Complex Field at Each Sensor from An Atmospheric Ray Model

Define the received complex baseband field for sensor m as the ray-traced steering component $a_m(\theta)$:

$$a_m(\theta) \triangleq G_m(\theta)\, \exp\Big(-j\, \Phi_m(\theta)\Big)\, \exp\Big(-\mathcal{A}_m(\theta)\Big)\, \Big(1 + \eta_m(\theta)\Big),$$

where the accumulated phase is

$$\Phi_m(\theta) = \int_0^{L_m(\theta)} k_0\, n\big(\mathbf{r}_m(\ell;\theta), t\big)\, d\ell + \phi_{m,\text{inst}},$$

and the accumulated attenuation is

$$\mathcal{A}_m(\theta) = \int_0^{L_m(\theta)} \alpha\big(\mathbf{r}_m(\ell;\theta), t\big)\, d\ell + a_{m,\text{inst}}.$$

Here $\phi_{m,\text{inst}}$ is an additive instrument phase offset and $a_{m,\text{inst}}$ is a receiver amplitude-loss term (both sensor-dependent constants or slowly varying calibrations). The term $\eta_m(\theta)$ is a complex perturbation capturing unmodeled scintillation and residual mismatch; a common small-error model is $\eta_m(\theta) \sim \mathcal{CN}(0, \sigma^2_{\eta,m})$.

This replaces the textbook narrowband plane-wave steering vector with a physically propagated steering vector that includes refraction and absorption.

18.3. Ray Equations with Atmospheric Refraction

Let the medium be characterized by $n(\mathbf{r}, t)$. A standard eikonal ray model uses

$$\frac{d\mathbf{r}}{ds} = \hat{\mathbf{t}}, \qquad \frac{d}{ds}\big(n\,\hat{\mathbf{t}}\big) = \nabla n,$$

where s is arc length and ∇n is evaluated at $\mathbf{r}(s)$. These equations define $\mathbf{r}_m(\ell;\,\theta)$ and $L_m(\theta)$ for each sensor given boundary conditions at the source or a chosen reference plane. In weak refraction, the straight-ray approximation uses $\mathbf{r}_m(\ell;\,\theta) \approx \mathbf{r}_0 + \ell\,\hat{\mathbf{u}}(\theta)$, and $L_m(\theta)$ is geometric.

18.4. MUSIC Projection with Ray-Traced Steering Components

Given the noise-subspace eigenvectors $u_{m,r}$ (from $\hat{\mathbf{R}}$), define

$$y_r(\theta) = \sum_{m=1}^{M} u^*_{m,r}\, a_m(\theta), \qquad r \in \{1, \ldots, M - \hat{K}\}.$$

With the ray-traced $a_m(\theta)$ above, this is explicitly

$$y_r(\theta) = \sum_{m=1}^{M} u^*_{m,r}\, G_m(\theta)\, \exp\Big(-j\,\Phi_m(\theta)\Big)\, \exp\Big(-\mathcal{A}_m(\theta)\Big)\, \Big(1 + \eta_m(\theta)\Big).$$

The denominator energy remains

$$d(\theta) = \sum_{r=1}^{M-\hat{K}} |y_r(\theta)|^2.$$

18.5. Atmospheric Error Terms and Finite-Sample Coupling

Separate deterministic and random contributions by writing

$$a_m(\theta) = \bar{a}_m(\theta)\,\Big(1 + \eta_m(\theta)\Big), \qquad \bar{a}_m(\theta) = G_m(\theta)\exp\big(-j\Phi_m(\theta)\big)\exp\big(-\mathcal{A}_m(\theta)\big).$$

Then

$$y_r(\theta) = \bar{y}_r(\theta) + \Delta y_r(\theta), \qquad \bar{y}_r(\theta) = \sum_{m=1}^{M} u_{m,r}^{*}\, \bar{a}_m(\theta), \qquad \Delta y_r(\theta) = \sum_{m=1}^{M} u_{m,r}^{*}\, \bar{a}_m(\theta)\, \eta_m(\theta).$$

A first-order expansion of the denominator is

$$d(\theta) = \sum_{r} |\bar{y}_r + \Delta y_r|^2 \approx \sum_{r} \left(|\bar{y}_r|^2 + 2\,\Re\{\bar{y}_r^{*} \Delta y_r\} \right),$$

with higher-order terms $\sum_r |\Delta y_r|^2$ retained when scintillation is not small. This term couples directly to the finitesnapshot perturbation of $\mathbf{U}_n$ because the estimated noise subspace depends on the same propagation impairments embedded in $\hat{\mathbf{R}}$.

18.6. Ray-Traced MUSIC Pseudospectrum With Atmospheric Terms

Define a stabilized pseudospectrum with floor $\epsilon > 0$:

$$P_{\mathrm{MUSIC}}(\theta) = \left[\max\left(\sum_{r=1}^{M-\hat{K}} \left| \sum_{m=1}^{M} u_{m,r}^{*}\, G_m(\theta)\, \exp\!\Big(-j \int_0^{L_m(\theta)} k_0\, n\big(\mathbf{r}_m(\ell;\theta), t\big)\, d\ell - j\, \phi_{m,\mathrm{inst}} \Big)\, \exp\!\Big(-\int_0^{L_m(\theta)} \alpha\big(\mathbf{r}_m(\ell;\theta), t\big)\, d\ell - a_{m,\mathrm{inst}} \Big)\, \big(1 + \eta_m(\theta)\big) \right|^2, \epsilon \right) \right]^{-1}.$$

This equation makes the mapping explicit.

The ray tracer provides $\mathbf{r}_m(\ell;\, \theta)$ and $L_m(\theta)$, and the atmospheric model provides $n(\mathbf{r}, t)$ and $\alpha(\mathbf{r}, t)$. MUSIC then applies the same noise subspace projection, but the steering vector is no longer geometric; it is a propagated field consistent with refraction and absorption.

18.7. Implementation Coupling to An Analytic Ray Tracer

Define per-sensor, per-angle ray integrals:

$$I_{n,m}(\theta; t) = \int_0^{L_m(\theta)} n\big(\mathbf{r}_m(\ell;\theta), t\big)\, d\ell, \qquad I_{\alpha,m}(\theta; t) = \int_0^{L_m(\theta)} \alpha\big(\mathbf{r}_m(\ell;\theta), t\big)\, d\ell.$$

Then

$$a_m(\theta) = G_m(\theta)\, \exp\Big(-j\, k_0\, I_{n,m}(\theta; t) - j\, \phi_{m,\mathrm{inst}} \Big)\, \exp\Big(-I_{\alpha,m}(\theta; t) - a_{m,\mathrm{inst}} \Big)\, \Big(1 + \eta_m(\theta)\Big).$$

This factorization isolates the ray-traced integrals from the subspace algebra and supports reuse strategies (compute $I_{n,m}$ and $I_{\alpha,m}$ once per (m, θ), then evaluate MUSIC sums for all r).

18.8. Notes on Atmospheric Content to Include

Refraction term: $n(\mathbf{r}, t)$ typically depends on temperature, pressure, and humidity (troposphere) or electron density (ionosphere). The ray equation uses ∇n.

Absorption term: $\alpha(\mathbf{r}, t)$ accounts for oxygen and water vapor absorption, rain/fog attenuation, and any frequencydependent terms. If frequency dependence matters across a bandwidth, replace k_0 and α with $k(\omega)$ and $\alpha(\omega)$ and integrate over ω after forming narrowband components.

Random term: $\eta_m(\theta)$ captures residual phase and amplitude scintillation and can be parameterized by structure functions or by a covariance model tied to C_n^2 (turbulence strength) when required.

19. Computational Complexity

This section analyzes the computational cost of the end-to-end MUSIC evaluation.

19.1. Computational Decomposition

The end-to-end cost per update is decomposed into dominant terms as

$$T_{\text{total}} = T_{\text{cov}} + T_{\text{EVD}} + T_{\text{scan}} + T_{\text{ray}} + T_{\text{misc}}.$$

Here T_{misc} includes mean removal, bookkeeping, peak picking, and optional curvature-based uncertainty. In most operating regimes T_{misc} is lower order and can be ignored for asymptotic scaling.

19.2. Covariance Construction Cost

Given N snapshots and M sensors, the sample covariance is

$$\hat{\mathbf{R}} = \frac{1}{N} \sum_{n=1}^{N} \mathbf{x}(n)\mathbf{x}^{H}(n).$$

Entrywise,

$$\hat{R}_{ij} = \frac{1}{N} \sum_{n=1}^{N} x_i(n) x_j^{*}(n), \qquad i, j \in \{1, \ldots, M\}.$$

A direct implementation forms all M^2 entries, each as a sum over N snapshots, yielding

$$T_{\text{cov}} = O(M^2 N).$$

Hermitian structure reduces constant factors by computing only the upper triangle and filling the lower triangle by conjugation, but the scaling remains $O(M^2 N)$.

19.3. Eigenvalue Decomposition Cost

A dense Hermitian eigendecomposition of an $M \times M$ matrix has cubic scaling

$$T_{\text{EVD}} = O(M^3).$$

This yields the eigenpairs and supports assembly of the noise-subspace matrix $\mathbf{U}_n \in \mathbb{C}^{M \times (M - \hat{K})}$ If only the noise subspace is needed, partial methods can reduce constants, but worst-case dense scaling remains $O(M^3)$.

19.4. MUSIC Scan Cost with Explicit Inner Products

For each scan angle $\theta \in \Theta$ and each noise mode $r \in \{1, \ldots, M - \hat{K}\}$, the core projection is

$$y_r(\theta) = \sum_{m=1}^{M} u_{m,r}^{*} a_m(\theta).$$

The denominator is

$$d(\theta) = \sum_{r=1}^{M - \hat{K}} |y_r(\theta)|^2.$$

Let the scan grid have $Q = |\Theta|$ angles. A direct evaluation computes $(M - \hat{K})$ inner products of length M per angle, so the arithmetic count scales as

$$T_{\text{scan}} = O\Big(Q\, M\, (M - \hat{K})\Big).$$

An equivalent matrix form is

$$\mathbf{y}(\theta) = \mathbf{U}_n^H \mathbf{a}(\theta), \qquad d(\theta) = \|\mathbf{y}(\theta)\|_2^2,$$

which makes it explicit that the per-angle cost is multiplication of an $(M - \hat{K}) \times M$ matrix by an $M \times 1$ vector.

19.5. Ray-Traced Steering Cost as Per-Angle, Per-Sensor Integration

With ray-traced steering, each steering component is computed as

$$a_m(\theta) = G_m(\theta)\, \exp\Big(- j\, k_0\, I_{n,m}(\theta; t) - j\, \phi_{m,\text{inst}} \Big)\, \exp\Big(- I_{\alpha,m}(\theta; t) - a_{m,\text{inst}} \Big)\, \Big(1 + \eta_m(\theta) \Big),$$

with ray integrals

$$I_{n,m}(\theta; t) = \int_0^{L_m(\theta)} n\big(\mathbf{r}_m(\ell; \theta), t\big)\, d\ell, \qquad I_{\alpha,m}(\theta; t) = \int_0^{L_m(\theta)} \alpha\big(\mathbf{r}_m(\ell; \theta), t\big)\, d\ell.$$

In a numerical implementation, each integral is approximated by L steps along the ray:

$$I_{n,m}(\theta; t) \approx \sum_{\ell=1}^{L} n\big(\mathbf{r}_{m,\ell}(\theta), t\big)\, \Delta s_\ell, \qquad I_{\alpha,m}(\theta; t) \approx \sum_{\ell=1}^{L} \alpha\big(\mathbf{r}_{m,\ell}(\theta), t\big)\, \Delta s_\ell,$$

where $\mathbf{r}_{m,\ell}(\theta)$ is the sample point at step ℓ for sensor m and direction θ, and Δs_ℓ is the step length (constant or adaptive).

Per (m, θ), two sums of length L are accumulated, plus a constant number of exponentials and multiplies. Therefore,

$$T_{\text{ray}} = O(Q\, M\, L).$$

19.6. Connecting L to Voxel Resolution and Modeled Area

Let the environment be represented as a voxel grid with voxel edge length Δ (meters). Let $D_m(\theta)$ be a representative geometric path length for sensor m and scan direction θ, and let D denote a representative path length scale.

If the ray integration samples the medium roughly once per voxel traversal, then

$$L(\theta, m) \approx \frac{D_m(\theta)}{\Delta}, \qquad L \approx \frac{D}{\Delta}.$$

Substituting into the ray cost yields

$$T_{\text{ray}} = O\left(Q\, M\, \frac{D}{\Delta} \right).$$

If the integration is adaptive, one may write

$$L \approx \int_0^{D} \frac{ds}{\Delta_{\text{eff}}(s)},$$

where $\Delta_{\text{eff}}(s)$ is an effective step length.

19.7. Full Per-Update Complexity

Collecting dominant terms gives

$$T_{\text{total}} = O(M^2 N) + O(M^3) + O\Big(Q\,M\,(M - \hat{K})\Big) + O(Q\,M\,L).$$

With voxelized propagation and $L \approx D/\Delta$,

$$T_{\text{total}} = O(M^2 N) + O(M^3) + O\Big(Q\,M\,(M - \hat{K})\Big) + O\left(Q\,M\,\frac{D}{\Delta}\right).$$

19.8. Regime Comparisons

Ray tracing dominates scan projection when

$$Q\,M\,L \gg Q\,M\,(M - \hat{K}) \quad \Longleftrightarrow \quad L \gg (M - \hat{K}).$$

Using $L \approx D/\Delta$,

$$\frac{D}{\Delta} \gg (M - \hat{K}).$$

Eigenanalysis dominates ray tracing when

$$M^3 \gg Q\,M\,L \quad \Longleftrightarrow \quad M^2 \gg Q\,L.$$

Using $L \approx D/\Delta$,

$$M^2 \gg Q\,\frac{D}{\Delta}.$$

19.9. Memory Footprint and Cache Implications for Voxel Fields

Let the voxel grid have dimensions $N_x \times N_y \times N_z$, so the total voxel count is

$$N_{\text{vox}} = N_x N_y N_z.$$

If both $n(\mathbf{r})$ and $\alpha(\mathbf{r})$ are stored as single-precision floats, the raw storage is approximately

$$B_{\text{fields}} \approx 8\,N_{\text{vox}} \text{ bytes}.$$

Ray integration is often memory-bandwidth limited because voxel accesses along rays are sparse and poorly contiguous, so cache misses can dominate runtime even when arithmetic scaling is $O(QML)$.

19.10. Reuse Structure and Precomputation

The computation can be factored as

$$\{I_{n,m}(\theta;t),\, I_{\alpha,m}(\theta;t)\}_{m,\theta} \implies \{a_m(\theta)\}_{m,\theta} \implies \{y_r(\theta)\}_{r,\theta} \implies \{d(\theta)\}_{\theta}.$$

If integrals are cached across updates, the per-update cost approaches

$$T_{\text{total}} \approx O(M^2 N) + O(M^3) + O\Big(Q\,M\,(M - \hat{K})\Big),$$

with integral refresh triggered only when atmospheric fields or geometry change beyond a tolerance.

20. Future Work

Future work will focus on controlled validation of the propagation-aware formulation. A primary comparison will evaluate plane-wave

MUSIC against ray-traced MUSIC under imposed refractive gradient profiles, including layered and continuously varying $n(\mathbf{r})$ fields derived from probe-laser measurements. The objective is to quantify bearing bias and resolution differences as a function of refractive curvature and vertical gradient magnitude. In addition, the bias and variance of the DOA estimate will be characterized as functions of turbulence strength, parameterized through structure constants and resulting phase perturbations. Sensitivity analysis will also examine peak displacement in the pseudospectrum as a function of modeling error in $n(\mathbf{r})$, explicitly relating steering-vector mismatch to systematic angular shift. These studies will establish the regimes in which ray-traced steering provides measurable improvement over geometric plane-wave assumptions and will bound the residual error attributable to imperfect atmospheric modeling.

21. Closing Comments

MUSIC is a subspace-based direction-of-arrival estimator that identifies signal directions by searching for steering vectors orthogonal to the noise subspace of the array covariance matrix. Its performance derives from eigenvalue separation between signal and noise components rather than direct power maximization. Resolution is governed by SNR, snapshot count, array calibration accuracy, and the stability of the covariance eigendecomposition, not by classical beamwidth limits alone.

A single summation-form expression for MUSIC exists by writing the pseudospectrum denominator as the squared norm of the steering vector projected onto the noise subspace. When expanded fully, it becomes a triple sum over noise-subspace modes and antenna indices. Once $\mathbf{U}_n$ is obtained from the eigendecomposition of $\hat{\mathbf{R}}$, the pseudospectrum evaluation reduces to deterministic nested summations and complex exponentials, with no remaining abstraction.

This framework extends directly to analytic ray tracing by replacing the conventional plane-wave steering vector a(θ) with a propagated steering vector computed from atmospheric path integrals. For each sensor m and candidate direction θ,

$$a_m(\theta) = G_m(\theta)\, \exp\Big(-j\,\Phi_m(\theta)\Big)\, \exp\Big(-\mathcal{A}_m(\theta)\Big)\, \Big(1+\eta_m(\theta)\Big),$$

with accumulated phase

$$\Phi_m(\theta) = \int_0^{L_m(\theta)} k_0\, n\big(\mathbf{r}_m(\ell;\theta),t\big)\, d\ell + \phi_{m,\mathrm{inst}}, \qquad k_0 = \frac{\omega_0}{c},$$

and accumulated attenuation

$$\mathcal{A}_m(\theta) = \int_0^{L_m(\theta)} \alpha\big(\mathbf{r}_m(\ell;\theta),t\big)\, d\ell + a_{m,\mathrm{inst}}.$$

Here $n(\mathbf{r}, t)$ is the refractive index field, $\alpha(\mathbf{r}, t)$ is specific attenuation in nepers per meter, $\mathbf{r}_m(\ell; \theta)$ is the ray trajectory, $L_m(\theta)$ is the path length to sensor m , $G_m(\theta)$ represents calibrated element gain and pattern, and $\eta_m(\theta)$ is a residual complex perturbation capturing scintillation and unmodeled effects.

Under this substitution, the MUSIC denominator remains

$$d(\theta) = \sum_{r=1}^{M-\hat{K}} \left| \sum_{m=1}^{M} u_{m,r}^{*}\, a_m(\theta) \right|^2,$$

but each steering component now embeds refraction, absorption, and instrument calibration. The eigendecomposition and noise-subspace projection machinery are unchanged; only the forward propagation operator inside $a_m(\theta)$ is modified.

Several operational advantages follow.

First, propagation effects that would otherwise appear as systematic steering mismatch are moved into the modeled term $\Phi_m(\theta)$ and $\mathcal{A}_m(\theta)$. This reduces bias in the pseudospectrum and prevents atmospheric structure from being misinterpreted as subspace noise.

Second, deterministic propagation and stochastic residual error are separated explicitly. The random term $\eta_m(\theta)$ can be parameterized and bounded, while deterministic phase curvature from refractive gradients is treated through the ray integral rather than absorbed into covariance perturbations.

Third, the computational structure remains clean. The expensive operations are the path integrals defining $\Phi_m(\theta)$ and $\mathcal{A}_m(\theta)$. These can be computed once per sensor and scan angle, then reused across all noise-mode projection sums. The covariance eigenanalysis remains a one-time operation per update cycle.

Finally, the estimator becomes propagation-aware without sacrificing the super-resolution properties of subspace methods. The algorithm continues to exploit eigenvalue separation for discrimination, but the steering hypothesis tested against the noise subspace is consistent with atmospheric physics rather than restricted to a geometric far-field approximation.

The result is a DOA estimator that preserves MUSIC's subspace resolution characteristics while incorporating refractive and absorptive structure directly into the forward model. This alignment between covariance eigenanalysis and analytic ray tracing is operationally important when environmental propagation is not negligible relative to aperture-induced phase structure.

References

1. Schmidt, R. (1986). Multiple emitter location and signal parameter estimation. *IEEE transactions on antennas and propagation, 34*(3), 276-280.
2. Pisarenko, V. F. (1973). The retrieval of harmonics from a covariance function. *Geophysical Journal of the Royal Astronomical Society, 33*(3), 347-366.
3. Bienvenu, G., & Kopp, L. (1983). Optimality of high resolution array processing using the eigensystem approach. *IEEE Transactions on acoustics, speech, and signal processing, 31*(5), 1235-1248.
4. Stoica, P., & Nehorai, A. (1989). MUSIC, maximum likelihood, and Cramer-Rao bound. *IEEE Transactions on Acoustics, speech, and signal processing, 37*(5), 720-741.
5. Van Trees, H. L. (2002). *Optimum array processing: Part IV of detection, estimation, and modulation theory*. John Wiley & Sons.
6. Kalman, R. E. (1960). A new approach to linear filtering and prediction problems. *Journal of Basic Engineering, 82*(1), 35-45.
7. Kay, S. M. (1993). Fundamentals of Statistical Signal Processing, Volume I: Estimation Theory. Prentice Hall.